Statistical analysis of the enhancement of tetrahedral carbon hybridization in amorphous carbon films produced from low-pressure radio-frequency plasma discharges

D. Wan and K. Komvopoulos

Department of Mechanical Engineering, University of California, Berkeley, California 94720

Abstract

A statistical analysis of the effect of Ar^+ bombardment on tetrahedral hybridization (sp^3) in amorphous carbon (a-C) thin films is presented for low-pressure radio-frequency (rf) plasma discharges. The model is based on a series of sequential events involving Ar^+ and carbon atom collisions at the surface of the growing film, followed by collisions between excited carbon atoms and other surface carbon atoms that enhance the formation of sp^3 bonding. Inelastic interactions (electronic stopping) of carbon atoms control the formation of sp^3 bonding via a cascade collision process involving inelastic interactions between carbon atoms. Atomic collisions are partly enhanced by elastic interactions (nuclear stopping) of Ar^+ and carbon atoms at the film surface. The model is validated by transmission electron and electron energy loss spectroscopy results revealing the existence of a two-layer film structure consisting of an ultrathin interface layer and the bulk of the film, without a surface layer rich in trigonal carbon hybridization (sp^2), as predicted by the subplantation model. Analytical results for the sp^3 carbon content are shown to be in good agreement with experimental results obtained from the analysis of the C 1s core level spectra of rf sputtered a-C films.

Submitted *to Physical Review Letters* on Sept. 23, 2003; revised manuscript submitted on Jan. 12, 2004.

Carbon can exist in three different hybridizations, i.e., tetrahedral, trigonal, and linear carbon bonding (referred to as sp^3, sp^2, and sp^1, respectively) and may form various crystalline and disordered structures. Since the synthesis of diamondlike carbon (dlc) films by ion beam deposition,[1] numerous deposition methods have been developed to produce dlc films[2] with properties varying between those of the two most common carbon allotropes, i.e., graphite (stable phase) and diamond (metastable phase).[3] An important characteristic of dlc films is the sp^3 carbon content that is strongly depended on the deposition conditions. Nonhydrogenated amorphous carbon (a-C) films rich in sp^3 bonded carbon, often referred to as tetrahedral amorphous carbon (ta-C) films, can be produced from energetic carbon ions using different techniques, such as mass-selected ion beam,[4-6] filtered cathodic vacuum arc,[7-10] and laser ablation.[11]

A common feature in ta-C films is the relatively high compressive residual stress. The formation of ta-C has been examined in the context of a compressive stress model based on the pressure-temperature phase diagram of carbon.[12] However, a study of published experimental data revealed that the compressive residual stress cannot be directly related to the sp^3 content of ta-C films.[13] The sp^3 hybridization in ta-C films induced by the bombardment of energetic carbon ions is a physical process that can be explained by the subplantation model.[5,14-17] The promotion of sp^3 bonding over the more stable structure of sp^2 bonding in ta-C films can be described by a model based on the mechanisms of shallow ion implantation and relaxation. According to this model, a very thin sp^2 hybridized layer is produced at the surface of ta-C films, and the film cross-section exhibits a three-layer structure consisting of the interface layer, the bulk of the ta-C film, and the sp^2 hybridized surface layer, used as a measure of the ion penetration depth, with thickness varying between 4 ± 2 and 13 ± 3 Å for corresponding ion energy of 35 and 320 eV.[18]

Carbon films with high sp^3contents can also be produced from low-pressure radio-frequency (rf) plasma discharges. The application of an optimum negative substrate bias voltage during rf sputtering promotes the development of a-C films exhibiting sp^3 contents as high as ~50 at.%. Because the film precursors in rf sputtering are low-energy (~10 eV) neutral carbon atoms, film densification results from the Ar^+ bombarding the surface of the growing film. The content of the implanted Ar^+ atoms in rf sputtered a-C films is typically less than 3 at.%,[19] suggesting that film penetration by the heavy Ar^+ is very small and that interactions between Ar^+ and carbon atoms occur mainly at the film surface, with most Ar^+ being backscattered from the surface. As a consequence, the film cross-section exhibits only a two-layer structure comprising the interface layer and the bulk of the a-C film.

To verify the existence of the above two-layer model in low-pressure rf plasma discharges and ion bombardment energy in the range of 60-210 eV, high-resolution transmission electron microscopy (TEM) studies were performed in a TEM (Philips CM300FEG/UT) with native resolution of 1.7 Å. The films were deposited on Si(100) substrates in a rf sputtering system (Perkin-Elmer Randex-240) without magnetron by Ar^+ sputtering a pure graphite target under forwarded rf power of 300 and 750 W and substrate bias of -200 V (i.e., ~210 eV Ar^+ bombarding energy). Figure 1 shows a high-resolution cross-section TEM image of an a-C film deposited at 300 W forwarded rf power and -200 V substrate bias voltage. According to the subplantation model, a layer with predominantly sp2 carbon bonding and thickness ~10 Å should exist at the film surface. However, only a two-layer film consisting of ~32 Å thick interface layer and ~77 Å thick uniform a-C layer can be seen in Fig. 1. A similar result was obtained for the a-C film deposited at 750 W forwarded rf power and –200 V substrate bias.

To further examine the existence of a two-layer film structure, electron energy loss spectroscopy (EELS) was performed with analytical TEM (Philips CM200FEG) having a spatial resolution of 10 Å and Gatan imaging filter with energy resolution of 0.9 eV. Figure 2 shows EELS spectra obtained from three different regions, i.e., interface, bulk, and surface of the a-C film shown in Fig. 1. Corresponding differential EELS spectra are shown in the insets of Fig. 2. The EELS spectrum obtained from the interface differs from that obtained from the center-region of the film. However, the EELS spectrum obtained from near the surface is almost the same as that obtained from the bulk of the film. The comparison of the EELS spectra obtained from the interface, bulk, and surface regions of the a-C film suggests that the cross-section of this film is a two-layer structure. The same conclusion was reached after comparing the EELS spectra of the a-C film deposited under 750 W forwarded rf power and –200 V substrate bias. In view of the obtained TEM and EELS results, the statistical nature of the sputtering process, and the presence of the heavy Ar^+, it may be inferred that the mechanisms of sp^3 carbon hybridization in sputtered a-C films differ significantly from those encountered in carbon films synthesized from highly energetic carbon ions, such as those produced by cathodic vacuum arc deposition, where the deposition conditions lead to the formation of a three-layer film structure (subplantation model).

The objective of this study, therefore, was to perform a statistical analysis of the effect of Ar^+ bombardment on the enhancement of sp^3 hybridization in sputtered a-C films. It is assumed that collisions occur between Ar^+ and carbon atoms at the film surface, and that these collisions promote the formation of sp^3 carbon bonding by a cascade collision process. The dissipation of the Ar^+ kinetic energy through ion-solid interactions is attributed to both nuclear collisions, where a fraction of the ion kinetic energy is transferred to carbon atom kinetic energy (elastic collisions), and electronic collisions, where a fraction of the ion kinetic energy is used to excite or eject carbon

atom electrons.[20] The corresponding interaction strengths depend on the nuclear and electronic stopping cross-sections.

The formation of sp^3 carbon bonding in sputtered a-C films due to the Ar^+ bombardment is considered to be a manifestation of the following sequential events.

Event A. An Ar^+ collides with a carbon atom (C1) at the surface of the sputtered a-C film. The probability of event A is $P(A)$.

Event B. Carbon atom (C1) at the film surface is excited due to the collision with the Ar^+. The probability of event B is proportional to the electronic stopping cross-section S_e, i.e., $P(B) \propto S_e(E_{Ar^+})$, where E_{Ar^+} is the Ar^+ kinetic energy. According to the Lindhard-Scharff electronic stopping cross-section model,[20] the probability of event B can be written as

$$P(B) = k_B E_{Ar^+}^{1/2} \quad , \tag{1}$$

where k_B is a proportional factor.

Event C. The excited carbon atom (C1) excites another carbon atom (C2) via a cascade collision process. The probability of event C is proportional to the electronic stopping cross-section, i.e., $P(C) \propto S_e\left(E_{C1}\right)$, where E_{C1} is the kinetic energy of the excited carbon atom C1, and can be written as[20]

$$P(C) \propto E_{C1}^{1/2} . \tag{2}$$

The kinetic energy of the excited carbon atom C1 due to event A is proportional to the nuclear stopping cross-section $S_n(E_{Ar^+})$ given by[20]

$$S_n(E_{Ar^+}) = \frac{C_m E_{Ar^+}^{1-2m}}{1-m} \left[\frac{4M_{Ar}M_C}{(M_{Ar}+M_C)^2}\right]^{1-m} , \tag{3}$$

where M_{Ar} and M_C are the atomic weights of the argon and carbon atoms, respectively, and C_m is a constant that depends on the value of the fit variable m. Using the Thomas-Fermi screen function, the values of m corresponding to various regions of reduced energy $\boldsymbol{e}$ are:[21] $m = 1/3$ for $\boldsymbol{e} \le 0.2$, $m = 0.5$ for $0.08 \le \boldsymbol{e} \le 2$, and $m = 1$ (Rutherford scattering) for $\boldsymbol{e} \ge 10$, where $\boldsymbol{e}$ is defined as

$$\boldsymbol{e} = \frac{M_C}{M_{Ar} + M_C} \frac{a_{TF}}{Z_{Ar} Z_C e^2} E_{Ar^+} \quad , \tag{4}$$

where Z_{Ar} and Z_C are the argon and carbon atomic numbers, respectively, e^2 = 1.44 eV-nm, and a_{TF} is the Thomas-Fermi screening length, defined as

$$a_{TF} = \frac{0.885 a_o}{(Z_{Ar}^{1/2} + Z_C^{1/2})^{2/3}} \quad , \tag{5}$$

where a_o = 0.05292 nm (Bohr radius). For Ar^+ bombardment on a sputtered a-C film with kinetic energy E_{Ar^+} < 1 keV, Eq. (4) yields $\boldsymbol{e} < 0.02$; hence, m = 1/3.[21] Therefore, the kinetic energy of the excited carbon atom C1 can be expressed as $E_{C1} \propto E_{Ar^+}^{1/3}$, and the probability of event C can be expressed as

$$P(C) = k_C E_{Ar^+}^{1/6} \quad , \tag{6}$$

where k_C is a proportionality factor.

Since the formation of sp^3 carbon bonding depends on the joint event $A \cap B \cap C$, the sp^3 percentage is proportional to the probability of the joint event $A \cap B \cap C$ and the total number of collisions between Ar^+ and carbon atoms at the a-C film surface *N*; thus

$$\frac{sp^3}{sp^2 + sp^3} \propto NP(A \cap B \cap C) \quad . \tag{7}$$

The probability of the joint event $A \cap B \cap C$ can be written as

$$P(A \cap B \cap C) = P(A \cap B) P(C | A \cap B) \quad , \tag{8}$$

where probability $P(C | A \cap B)$ is given by

$$P(C | A \cap B) = \frac{P(C) P(A \cap B | C)}{P(A \cap B)} \quad . \tag{9}$$

If $P(C) \neq 0$, then $P(A \cap B | C) =$ 1, and Eqs. (6), (8), and (9) give that the probability of the joint events $A \cap B \cap C$ is

$$P(A \cap B \cap C) = P(C) = k_C E_{Ar^+}^{1/6} \, . \tag{10}$$

The total number of collisions between Ar^+ and carbon atoms at the film surface is proportional to the sum of the impinging particle fluxes

$$N \propto J_C + J_{Ar^+} \quad , \tag{11}$$

where J_C and J_{Ar^+} are the fluxes of impinging neutral carbon atoms and Ar^+, respectively. In view of the interdependence of the above particle fluxes,

$$J_C \propto \boldsymbol{g} J_{Ar^+} \quad , \tag{12}$$

where $\boldsymbol{g}$ is the carbon atom sputtering yield due to the Ar^+ bombardment on the pure graphite target surface, Eqs. (7) and (10)-(12) yield that the fraction of sp^3 bonded carbon atoms is

$$\frac{sp^3}{sp^2 + sp^3} = k J_{Ar^+} E_{Ar^+}^{1/6} \, , \tag{13}$$

where k is a proportionality factor.

To verify the validity of the above model, experimental results were obtained for thin a-C films deposited on Si(100) substrates under conditions of forwarded rf power in the range of 298-755 W, substrate bias voltage between –50 and –200 V, Ar gas flow rate of 20 sccm, working

pressure of 3 mTorr, and deposition time equal to 3 min. The substrate temperature was maintained at room temperature by a cooling system. Based on energy balance considerations, the Ar^+ impinging flux J_{Ar^+} is given by

$$J_{Ar^+} = \frac{P_a}{qA(2V_p - V_T - V_S)} \quad , \tag{14}$$

where q is the electron charge, V_p is the time-averaged plasma bulk voltage (≈ 10 V), V_T and V_S are the time-averaged voltages at the target and substrate surfaces, respectively, P_a is the absorbed rf power, and A is the surface area of the substrate holder (8-inch-dia. target surface area for a symmetrical rf discharge geometry configuration).

X-ray photoelectron spectroscopy (XPS) studies of the a-C film surfaces were carried out in a high-vacuum XPS system (PHI Model 5400). Gaussian-Lorentzian (GL) profiles were fit to the C 1s XPS spectra using a standard least-squares algorithm, after subtracting the background noise based on the Shirley method.[22] Díaz et al.[23] reported that the line positions of sp^2 and sp^3 hybrids are at 284.3 eV and 285.2 eV, respectively, in C 1s spectra of a-C films deposited by pulsed laser evaporation of graphite targets, and that the binding energy of the sp^3 hybrids is upward shifted by 0.9 eV from that of the sp^2 hybridized carbon. Jackson et al.[24] reported that the binding energies of 284.84 eV and 285.80 eV correspond to sp^2 and sp^3 bonded carbons, respectively, in a-C films deposited by dc magnetron sputtering and cathodic arc deposition. Taki and Takai[25] observed sharp peaks at 284.15 eV and 285.50 eV in the spectra of graphite and diamond, respectively, and assigned these values to the binding energies of sp^2 and sp^3 bonded carbon in a-C:H films synthesized by shielded arc ion plating. They also reported that the corresponding full-width at half-magnitude (FWHM) values are equal to 1.0 and 2.20 eV. Mérel et al.[26] found that the binding energies of sp^2 and sp^3 hybridized carbon atoms in pulsed laser deposited a-C films are at 284.4 eV

and 285.2 eV, respectively, and that the corresponding FWHM values are equal to 1.0 and 1.10 eV. Tay et al.[27] found that the line positions of sp^2 and sp^3 bindings in a-C films deposited by the filtered cathodic vacuum arc are at 284.3 and 285.1 eV, respectively. Lu and Komvopoulos[28,29] reported that the binding energies of sp^2 and sp^3 hybridized carbon atoms in a-C films deposited by rf sputtering are in the ranges of 284.24-284.45 eV and 285.36-285.44 eV, respectively, depending on the deposition conditions.

In view of the above investigations, the search of the sp^2 and sp^3 binding peak positions in this study was performed in the ranges of 283.95-284.55 and 284.95-285.70 eV, respectively, while the sp^1 binding peak position was searched in the range of 282-283.5 eV. To account for the effect of oxygen atoms from the ambient, three additional peaks were searched in the ranges of 286-287, 287-288.5, and 288.5-290.5 eV, respectively.[29] Hence, six GL profiles were used to fit the C 1s core level XPS spectra. FWHM values of all the XPS peaks were obtained in the range of 0-3 eV. Figure 3 shows a representative C 1s core level XPS spectrum of the produced rf sputtered a-C films with six Gaussian-Lorentzian profile fits. Experimental results for the sp^3 carbon content of various rf sputtered a-C films (determined from the analysis of corresponding C 1s XPS spectra) in terms of deposition conditions are given in Table I. Figure 4 shows the percentage of sp^3 bonded carbon atoms in a-C films sputtered under different deposition conditions versus $J_{Ar^+} E_{Ar^+}^{1/6}$. The experimental data are in good agreement (correlation factor, R^2 = 0.8715) with the predictions of the statistical model (Eq. 13). The favorable comparison of the analytical and TEM, EELS, and XPS results confirms that the enhancement of the sp^3 carbon hybridization in rf sputtered a-C films is mainly due to the effect of Ar^+ bombardment.

The present study demonstrates that a series of sequential events involving Ar^+ and carbon atom collisions at the surface of the growing film, followed by collisions between the excited

carbon atoms and other surface carbon atoms are responsible for the enhancement of sp^3 carbon bonding in rf sputtered a-C films. The sp^3 carbon hybridization is mainly due to the inelastic interactions of atomic carbon (electronic stopping) that promote the formation of sp^3 bonding via a collision cascade process, assisted by elastic interactions of Ar^+ and carbon atoms at the film surface. The atomic collisions are partly enhanced by elastic interactions (nuclear stopping) of Ar^+ and carbon atoms at the film surface. Analytical results show that the sp^3 carbon content in sputtered a-C films is linearly proportional to $J_{Ar^+} E_{Ar^+}^{1/6}$, which is in good agreement with experimental results obtained from the analysis of the C 1s core level spectra of rf sputtered a-C films.

This research was supported by the National Science Foundation under Grant No. CMS-9734907, and the Computer Mechanics Laboratory at the University of California at Berkeley.

[1]S. Aisenberg and R. Chabot, J. Appl. Phys. **42**, 2953 (1971).

[2]J. Robertson, Mater. Sci. Eng. **R37**, 129 (2002).

[3]J. E. Field, *Properties of Diamond* (Academic, London, UK, 1979).

[4]J. Ishikawa, Y. Takeiri, K. Ogawa, and T. Takagi, J. Appl. Phys. **61**, 2509 (1987).

[5]Y. Lifshitz, S. R. Kasi, J. W. Rabalais, and W. Eckstein, Phys. Rev. B **41**, 10468 (1990).

[6]Y. Lifshitz, G. Lempert, and E. Grossman, Phys. Rev. Lett. **72**, 2753 (1997).

[7]D. R. McKenzie, D. Muller, and B. A. Pailthorpe, Phys. Rev. Lett. **67**, 773 (1991).

[8]P. J. Fallon, V. S. Veerasamy, C. A. Davis, J. Robertson, G. A. J. Amaratunga, W. I. Milne, and J. Koskinen, Phys. Rev. B **48**, 4777 (1993).

[9]G. Jungnickel, M. Kuhn, S. Deutschmann, F. Richter, U. Stephan, P. Blaudeck, and T. Frauenheim, Diamond Rel. Mater. **3**, 1056 (1994).

[10]S. R. P. Silva, S. Xu, B. X. Tay, H. S. Tan, and W. I. Milne, Appl. Phys. Lett. **69**, 491 (1996).

[11]P. Kovarik, E. B. D. Bourdon, and R. H. Prince, Phys. Rev. B **48**, 12123 (1993)

[12]D. R. McKenzie, D. Muller, and B. A. Pailthorp, Phys. Rev. Lett. **67**, 773 (1991).

[13]A. C. Ferrari, S. E. Rodil, J. Robertson, and W. I. Milne, Diamond Rel. Mater. **11**, 994 (2002).

[14]Y. Lifshitz, S. R. Kasi, and J. W. Rabalais, Phys. Rev. Lett. **62**, 1290 (1989).

[15]J. Robertson, Diamond Rel. Mater. **3**, 361 (1994).

[16]J. Robertson, Diamond Rel. Mater. **5**, 519 (1996).

[17]H. Hofsäss, H. Feldermann, R. Merk, M. Sebastian, and C. Ronning, Appl. Phys. A **66**, 153 (1998).

[18]C. A. Davis, G. A. J. Amaratunga, and K. M. Knowles, Phys. Rev. Lett. **80**, 3280 (1998).

[19]W. Lu and K. Komvopoulos, Appl. Phys. Lett. **76**, 3206 (2000).

[20]M. Nastasi, J. W. Mayer, and J. K. Hirvonen, *Ion-Solid Interactions: Fundamentals and Applications*, Ch. 5 (Canbridge University Press, Cambridge, UK, 1996).

[21]K. B. Winterbon, P. Sigmund, and J. B. Sanders, Mat. Fys. Medd. Dan Vid. Selsk. **37**, 1 (1970).

[22]D. A. Shirley, Phys. Rev. B **5**, 4709 (1972).

[23]J. Díaz, G. Paolicelli, S. Ferrer, and F. Comin, Phys. Rev. B **54**, 8064 (1996).

[24]S. T. Jackson and R. G. Nuzzo, Appl. Surf. Sci. **90**, 195 (1995).

[25]Y. Taki and O. Takai, Thin Solid Films **316**, 45 (1998).

[26]P. Mérel, M. Tabbal, M. Chaker, S. Moisa, and J. Margot, Appl. Surf. Sci. **136**, 105 (1998).

[27]B. K. Tay, X. Shi, H. S. Tan, and D. H. C. Chua, Surf. Interf. Anal. **28**, 231 (1999).

[28]W. Lu and K. Komvopoulos, J. Appl. Phys. **85**, 2642 (1999).

[29]W. Lu and K. Komvopoulos, J. Appl. Phys. **89**, 2422 (2001).

Table I Dependence of sp^3 carbon content on experimental rf sputtering conditions.*

Forwarded rf power, P_f (W)	Absorbed rf power, P_a (W)	Substrate bias, V_S (V)	Ion flux, J_{Ar^+} (X 10^{15} /s-cm^2)	$J_{Ar^+} E_{Ar^+}^{1/6}$ (X 10^{15} eV$^{1/6}$/s-cm^2)	$\frac{sp^3}{sp^2 + sp^3}$ (%)
299.5	282.5	-200	5.438	13.257	30.41
403.5	393.5	-200	6.234	15.199	33.77
499.5	495.5	-200	6.74	16.433	37.23
603	597	-200	7.366	17.959	42.2
755	752	-200	8.178	19.938	48.62
298.5	298.5	-50	5.37	10.625	27.24
299	299	-100	5.304	11.611	28.58
298	293	-150	5.371	12.515	30.73
754.5	749.5	-50	8.306	16.433	32.56
754.5	751.5	-100	8.266	18.093	38.79
754	754	-150	8.2	19.105	41.09

*Working pressure = 3 mTorr; Ar gas flow rate = 20 sccm; deposition time = 3 min.

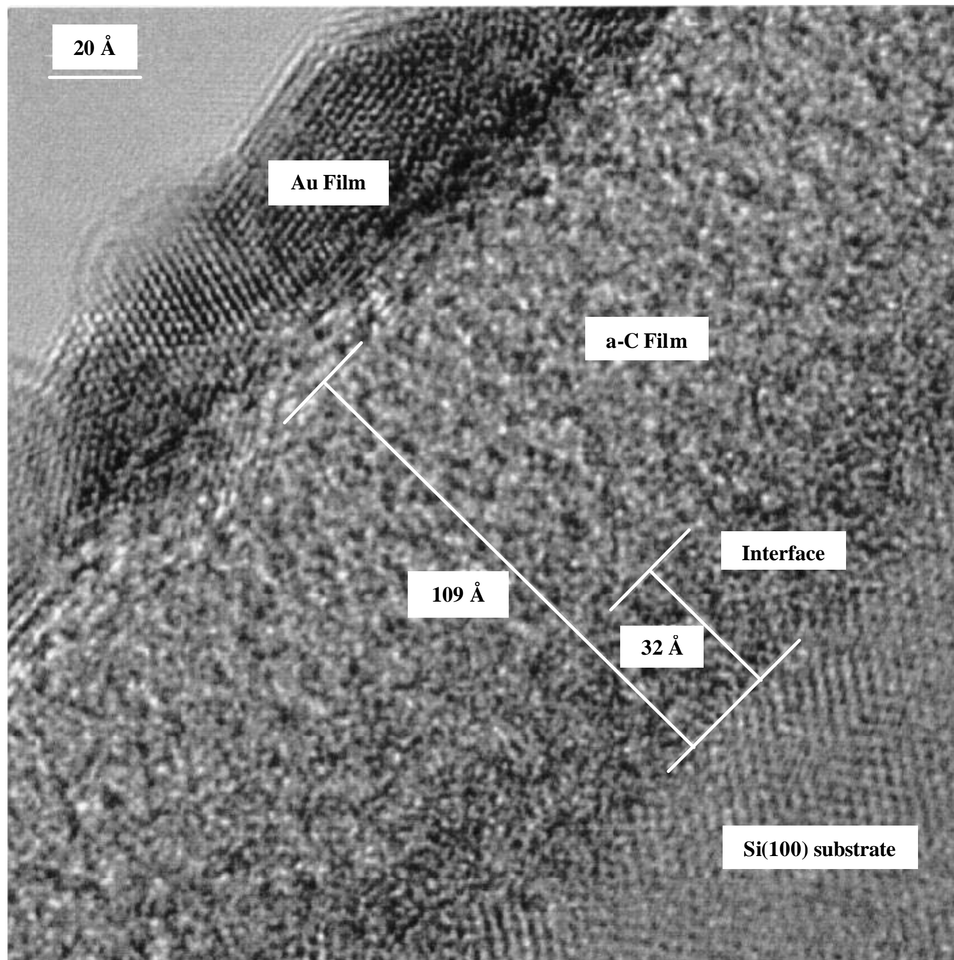

FIG. 1 High-resolution cross-section TEM image of a-C film deposited by rf sputtering under conditions of forwarded rf power of 300 W and substrate bias voltage of –200 V.

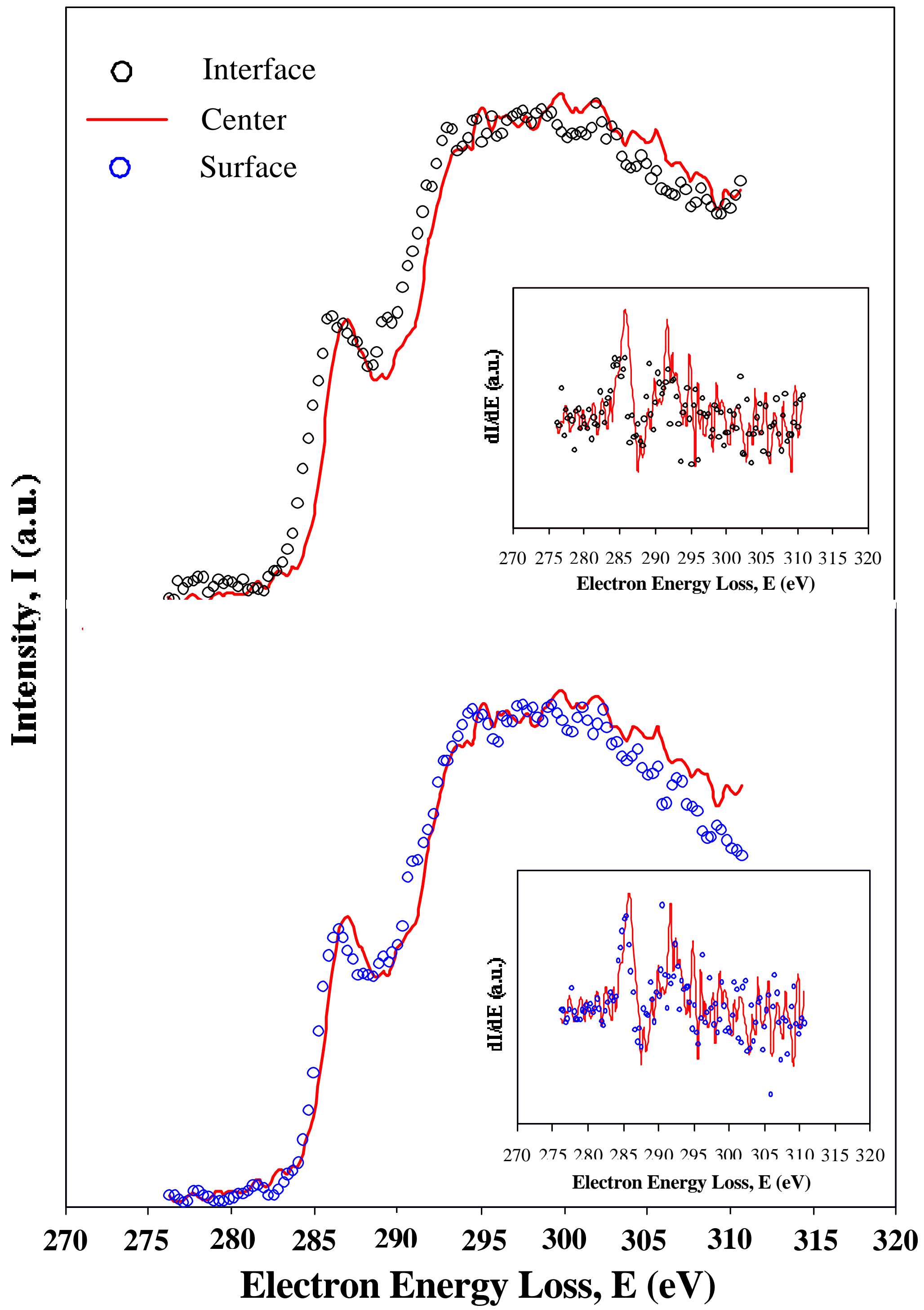

FIG. 2 EELS spectra obtained from a-C film deposited by rf sputtering under conditions of forwarded rf power of 300 W and substrate bias voltage of –200 V.

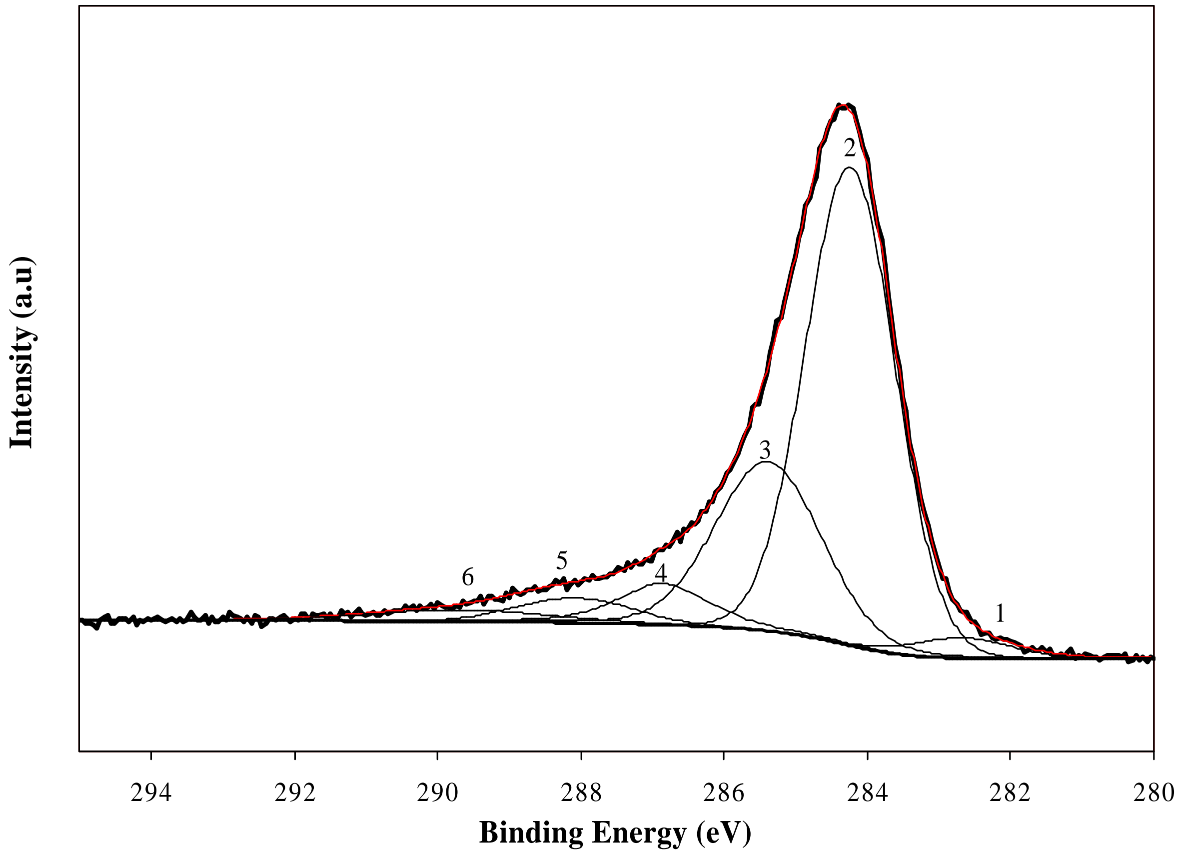

FIG. 3 Typical C 1s core level XPS spectrum of a-C films deposited by rf sputtering under conditions of forwarded rf power of 300 W and substrate bias voltage of –200 V with six Gaussian–Lorentzian profile fits.

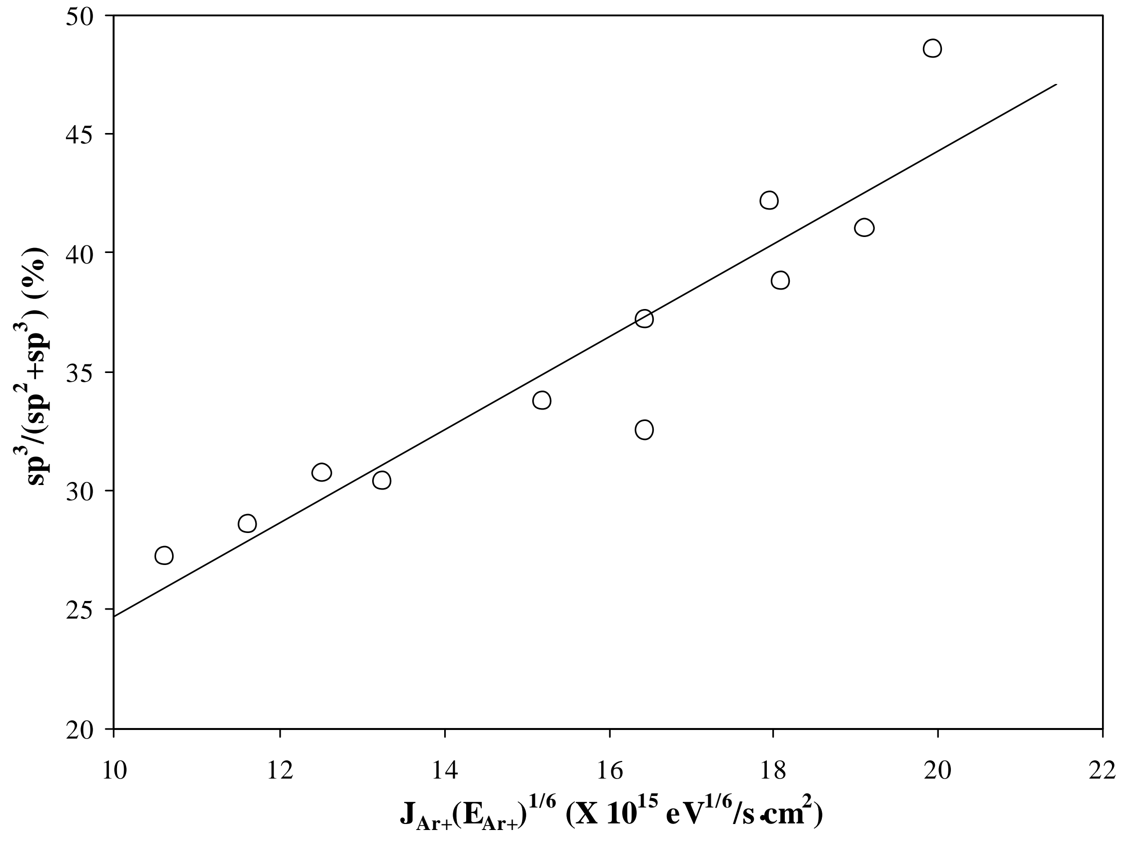

FIG. 4 Comparison of analytical and experimental results for the dependence of the sp^3 carbon content in rf sputtered a-C films on the Ar^+ impinging flux and kinetic energy.